Synthesis, Characterization and TheoreticalStudies of N'-(4-methoxybenzylidene)benzenesulfonohydrazide

[1]H. Güzin Aslan* and [2]Lütfiye Aydin
[1]*Erciyes University, Faculty of Science, 38039, Kayseri, Turkey.*
[2]*Kayseri Metropolitan Municipality, Head of Survey and Projects Department,Kayseri Turkey.*
guzina@erciyes.edu.tr*

(Received on 25th Feb 2020, accepted in revised form 2ndNovember)

Summary: N'-(4-methoxybenzylidene)benzenesulfonohydrazide was synthesized and elemental analysis was conducted; IR, Raman, ^{1}H, and ^{13}C NMR spectral data were recorded. The potential energy surfaces (PES) of the N'-(4-methoxybenzylidene)benzenesulfonohydrazide molecule were obtained by selected degree of torsional freedom, which varied from 0° to 360° in 4° increments. The conformers were optimized by using a (DFT/B3LYP/6-31G(d,p)) basis set in the gas phase. The eleven conformers in the gas phase of the obtained molecule were determined and the most stable conformer (conformer 1) was re-optimized by three different basis sets of 6-31G(d,p), 6-311G(d,p), and LanL2Dz.

HOMO-LUMO analyses were performed. NBO analysis was performed to describe the around of intramolecular charge transfer. The vibrational spectra were measured in solid phase IR and detailed analysis of the vibrational spectra of conformer 1 was done; all the bands of the spectra were interpreted by the use of the potential energy distributions (PED) and the molecular electrostatic potential (MEP) was plotted.

Keywords:Sulfonohydrazide, DFT, PES, NBO, Vibrational Analysis.

Introduction

Sulfa drugs were discovered by German bacteriologist and pathologist Gerhard Domagk. The scientist found that the active component of the prontosil dye was the sulfonyl amide. This discovery gave him the Nobel Prize in 1939 [1,2].

This type of drugs was used extensively during World War II [3].These drugs were in the form of white powder medicines taken orally and included inmilitary first aid equipment. Due to bacterial resistance, the use of these drugs has decreased over time. Today, their use as antibacterial drugs continues in the form of binary or triple mixtures. Sulfa drugs do not kill bacteria, but stop their reproduction and growth. Conversely, antibiotic drugs kill bacteria because the mechanism of action is different. Therefore, treatment with sulfamide drugs is preferred in many infections.

Sulfonylamides are important compounds for drug chemists. The many bioactive properties of these compounds such as anticancer [4], antidiabetic [5], anti-inflammatory [4], antifungal [6], antibacterial [7], antituberculosis [8,9], antiviral [10], and glycosidase inhibition [11]have been reported.

Computational methods are useful for detecting various molecular properties [12]. These studies are often used by researchers to verify experimental results [13]. These studies provide a pool of information for those who want to work on such compounds with a wide range of uses.

This study has synthesized N'-(4-methoxybenzylidene)benzenesulfonohydrazide in order to give a different perspective to this group of compounds, which have a wide use area. After synthesization, spectroscopic methods from previous studies were used to characterize it [14,15].

Vibrational frequencies [16], LUMO-HOMO energies [17], frontier orbital energy gap [18], dipole moment, and NBO analysis [19] were employed. Infrared and NMR spectroscopic methods are widely used to study the structural and dynamic properties of molecular systems [20]. Detailed DFT calculations were made and compared with the experimental results.

The vibrational bands in the IR and Raman spectra were assigned by normal coordinate analysis (NCA) and were interpreted by theoretical calculations using three different basis sets.

*To whom all correspondence should be addressed.

Experimental

General materials and instruments

The chemicals available on the market were used without purification. Solvents were distilled because the substance was affected by water. The melting point was determined with the melting point device (Elektrotermal 9100). The compound was routinely controlled by TLC using the DC AlufolienKieselgel 60 F254 (Merck) and the Camag TLC lamp (254/366 nm). IR spectra were recorded with the Shimadzu Model 8400 FT-IR spectrophotometer. The ^{1}H spectra were recorded with the Bruker 400 MHz NMR device and ^{13}C-NMR spectra were recorded with the Bruker 100 MHz NMR device.

General Procedure for the Preparation ofN'-(4-methoxybenzylidene)benzenesulfonohydrazide

The substance was synthesized by a method used in previous studies [21]. The light yellow product was re-crystallized from ethanol three times. This resulting solid was stable at normal conditions and soluble in ethanol. N'-(4-methoxybenzylidene) benzenesulfonohydrazide was obtained at a 55% yield as a light yellow mass($C_{15}H_{16}N_2SO_2$ 288.26): Anal Found: C, 64.96; H, 5.86; N, 10.15; S, 11.70% Calc.: C, 62.47; H, 5.59; N, 9.71; S, 11.12%. FT-IR (cm^{-1}): $\nu_{C\text{-}S,}$ 723, $\nu_{S\text{-}N,}$ 867, $\nu_{sSO2,}$1178, $\nu_{asSO2,}$ 1299, $\delta_{C\text{-}H,}$ 1460, $\nu_{C\text{-}Caro,}$ 1618, $\nu_{C\text{-}N,}$ 1654, $\nu_{s\ CH3,}$ 2902, $\nu_{as\ CH3,}$ 2925.^{1}H NMR (δ, ppm, 400 MHz, DMSO- d_6): 8.84 (s,^{1}H,N-CH), 8.64-7.16 (d, 9H, Ar-H), 4.05-3.49 (s, 6H, CH_3); ^{13}C NMR (100 MHz, (DMSO-d_6): δ= 162.10, 161.13,132.00,130.24, 126.82, 114.62, 114.28, 77.35,77.03, 76.71. The compounds' M.p.: 187 °C.

Computational Details

All the calculations were computed by the DFT method using the Gaussian 09 program [22] and GaussView05 program [22]. The reaction mechanism of the synthesized molecule is given in Fig **1.**

The initial geometry was generated from the standard geometrical parameters and theoretically investigated with the Density Functional Theory (DFT) using the B3LYP [23] hybrid exchange-correlation function. All the optimized structural parameters were obtained by re-optimizing the minima structures of the PES. Harmonic vibrational frequencies and their assignments were also computed using the same basis set.

The results of NBO analysis, optimized geometric, parametric and NMR spectra were calculated by the DFT/B3LYP 6-31G(d,p), 6-311G(d,p), and LanL2Dzbasis sets for the most stable conformer. Vibrational and frontier molecular orbital analysis of the most stable conformer was conducted with the DFT/B3LYP 6-31G(d,p) basis set. Potential energy distribution (PED) was performed with the VEDA4 [24] program and each band of the vibrational frequencies was interpreted.

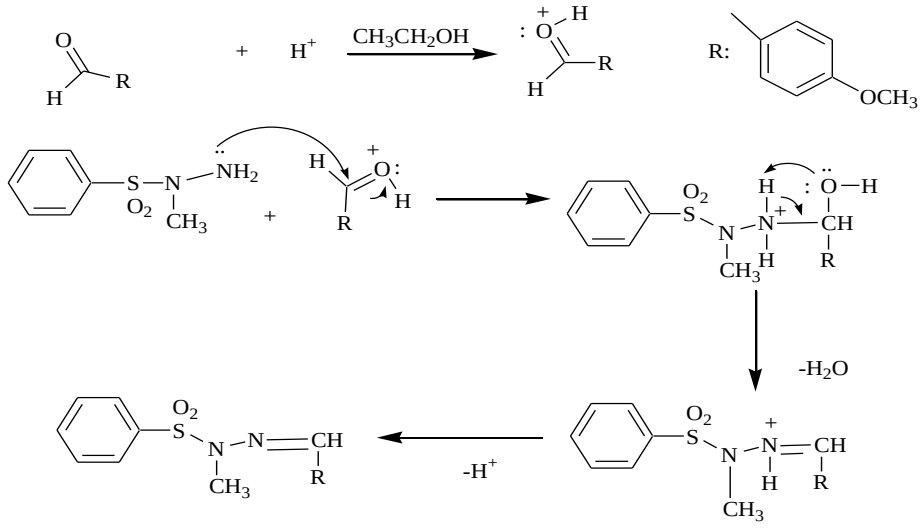

Fig. 1: The reaction mechanism of the synthesized molecule.

Results and Discussion

Potential energy surfaces

To find the conformers of the obtained molecule, a scan through of the eight torsional angle coordinates $\tau(C_2C_3S_{12}O_{12})$, $\tau(C_{19}N_{15}S_{12}O_{13})$, $\tau(N_{15}N_{16}C_{17}H_{18})$, $\tau(N_{16}N_{15}C_{19}H_{21})$, $\tau(N_{16}C_{17}C_{28}C_{23})$, $\tau(C_{25}O_{33}C_{34}H_{35})$, $\tau(C_{19}N_{15}C_{16}C_{17})$, and $\tau(C_{24}C_{25}O_{33}C_{34})$, was done. These torsion angles are shown in Fig 2.The potential energy surfaces were determined with a change in eight dihedral angles in intervals of 4°.

The relative energies of the eleven conformers of the obtained molecule were calculated by DFT with the 6-31G(d,p), 6-311G(d,p), and LanL2Dz basis sets. The highest rotational energy barrier in the gas phase was determined for the $N_{15}N_{16}C_{17}H_{18}$ angle with 48 kcal/mol. The lowest rotational barrier was calculated as 3 kcal/mol for the $N_{16}N_{15}C_{19}H_{21}$ angle. Some geometric parameters of the most stable conformer can be seen in Table 1, the eight torsion angles, which characterize the eleven conformers, can be seen in Table 2, and the geometries of the conformers can be seen in Fig 3.

The relative energy difference between the most stable conformer and the other 10 conformers was found to be 4 kcal/mol. The relative energy difference of 82 kcal/molwas found between the most stable conformer and conformer 11.

The highest rotational barrier was obtained for the rotation around the bonds $N_{16}S_{12}$ and $N_{15}C_{16}$. The value of this barrier was calculated to be 10 kcal/mol. The $N_{16}C_{17}$ bond could not scanned between 100-260 degrees due to overlap of the sulfonyl group and p-methoxy benzene ring.

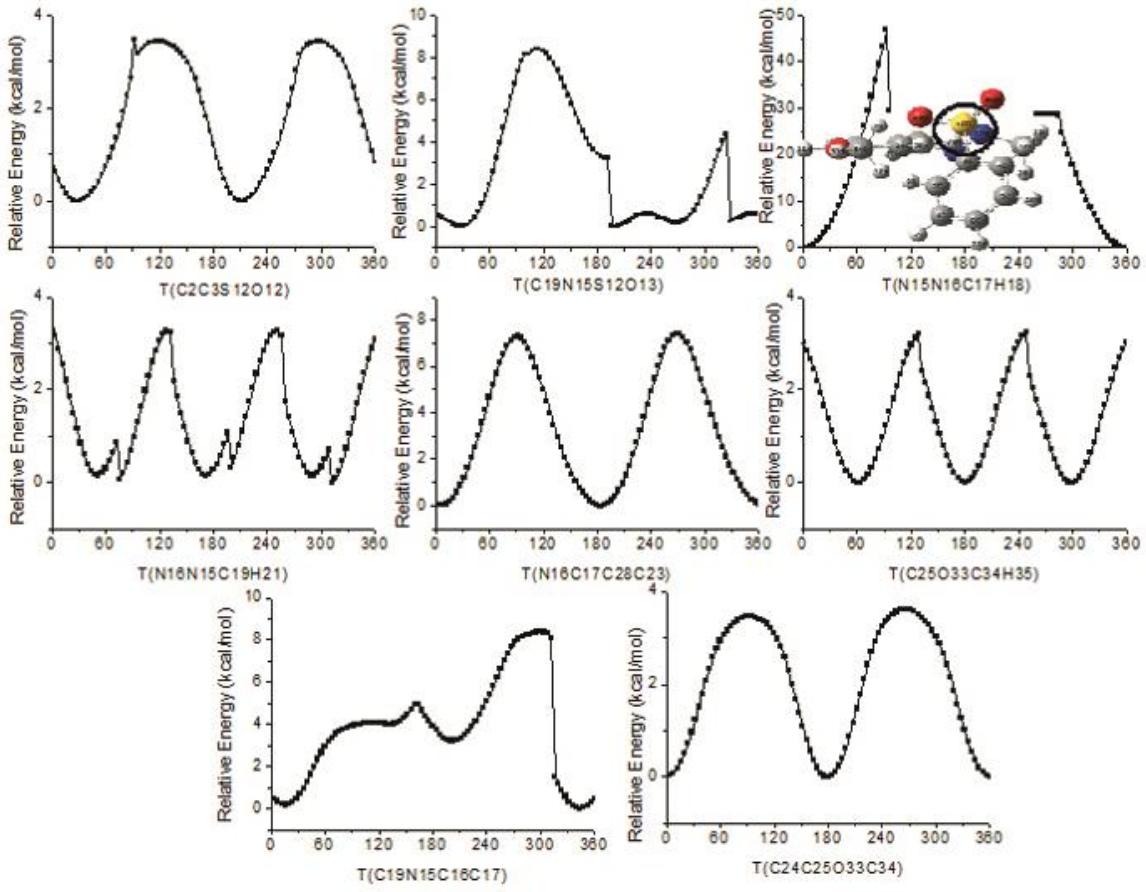

Fig 2: PES of the title compound.

Table 1: Some Optimized geometrical parameters of the most stable conformer.

Parameters	Calculated		
Bond lengths (Ao)	**6-31G(d,p)**	**6-311G(d,p)**	**Lan2-Dz**
C_3-S_{12}	1.79	1.80	1.86
S_{12}-O_{13}	1.47	1.46	1.63
S_{12}-O_{14}	1.46	1.45	1.63
S_{12}-N_{15}	1.73	1.72	1.89
$N_{15}N_{16}$	1.37	1.36	1.38
$N_{15}C_{19}$	1.46	1.46	1.48
N_{16}-C_{17}	1.29	1.28	1.31
C_{17}-H_{18}	1.09	1.09	1.09
C_{17}-C_{28}	1.46	1.46	1.47
C_{19}-H_{20}	1.10	1.10	1.10
C_{19}-H_{21}	1.09	1.09	1.10
C_{19}-H_{22}	1.09	1.09	1.09
C_{24}-H_{30}	1.08	1.08	1.09
O_{33}-C_{34}	1.42	1.42	1.46
$C_2C_3S_{12}$	119.3	119.3	117.9
$C_4C_3S_{12}$	119.0	119.1	118.0
$C_3S_{12}O_{13}$	108.2	108.2	109.7
$C_3S_{12}O_{14}$	108.3	108.4	108.6
$C_3S_{12}N_{15}$	105.6	105.1	101.2
$O_{13}N_{12}O_{14}$	122.2	122.3	120.5
$O_{13}N_{12}N_{15}$	104.5	104.5	102.7
$O_{14}S_{12}N_{15}$	106.9	107.1	112.2
$N_{16}N_{15}S_{12}$	111.4	111.7	108.7
$C_{19}N_{15}S_{12}$	119.1	119.0	113.9
$N_{16}N_{15}C_{19}$	122.2	122.3	123.1
$N_{15}N_{16}C_{17}$	120.3	120.6	121.1
$N_{16}C_{17}H_{18}$	122.7	122.6	122.3
$N_{16}C_{17}C_{28}$	121.1	121.2	121.3
$H_{18}C_{17}C_{28}$	116.2	116.1	116.4
$C_{25}C_{24}H_{30}$	121.1	121.1	121.2
$C_2C_3S_{12}$	119.3	119.3	117.9
$C_4C_3S_{12}$	119.0	119.1	118.0
$C_3S_{12}O_{13}$	108.2	108.2	109.7
$C_3S_{12}O_{14}$	108.3	108.4	108.6
$C_3S_{12}N_{15}$	105.6	105.1	101.2
$O_{13}S_{12}O_{14}$	122.2	122.3	120.5
$O_{13}S_{12}N_{15}$	104.5	104.5	102.7
$O_{14}N_{15}S_{12}$	106.9	107.1	112.2
$S_{12}N_{15}N_{16}$	111.4	111.7	108.7

Table-2: Computational relative energies, dipole moments, and flexible bonds of the PES minima.

Conformers	Rel.Energy(kcal/mol)	Dipolmoment (Debye)	$\tau(C_2C_3S_{12}O_{13})$	$\tau(C_{19}N_{15}S_{12}O_{13})$	$\tau(N_{15}N_{16}C_{17}H_{18})$	$\tau(N_{16}N_{15}C_{19}H_{21})$	$\tau(N_{16}C_{17}C_{28}C_{23})$	$\tau(C_{25}O_{33}C_{34}H_{35})$	$\tau(C_{19}N_{15}C_{16}C_{17})$	$\tau(C_{24}C_{25}O_{33}C_{34})$
Conf.1	**0**	**7.02**	**165.9**	**28.4**	**1.4**	**68.5**	**-175.3**	**61.4**	**-15.6**	**-0.4**
Conf.2	**0**	**7.03**	**165.9**	**28.4**	**1.4**	**68.5**	**4.8**	**61.4**	**-15.6**	**179.4**
Conf.3	**0.0028**	**5.52**	**167.8**	**29.7**	**1.69**	**-52.3**	**5.83**	**61.3**	**-15.5**	**0.2**
Conf.4	**0.1914**	**4.88**	**147.2**	**-160.7**	**-1.7**	**52.3**	**-5.8**	**61.1**	**15.6**	**-0.2**
Conf.5	**0.1914**	**4.88**	**162.0**	**-91.4**	**2.4**	**70.0**	**1.9**	**61.4**	**-16.6**	**-0.4**
Conf.6	**0.1914**	**4.88**	**148.9**	**-39.9**	**-2.3**	**50.9**	**-1.8**	**61.0**	**16.6**	**0.4**
Conf.7	**0.5933**	**6.41**	**165.8**	**50.8**	**0.3**	**63.7**	**1.2**	**61.7**	**-152.7**	**-0.6**
Conf.8	**3.2217**	**4.13**	**135.5**	**-167.7**	**1.6**	**66.0**	**-1.6**	**61.2**	**-15.6**	**-0.1**
Conf.9	**3.2300**	**4.90**	**117.2**	**-26.9**	**4.9**	**70.3**	**1.8**	**61.5**	**-157.8**	**-0.4**
Conf.10	**4.0219**	**6.44**	**144.3**	**-54.7**	**-0.2**	**51.2**	**-1.8**	**61.2**	**133.2**	**0.2**
Conf.11	**82.5603**	**4.06**	**-147.7**	**92.2**	**-1.1**	**51.8**	**0.6**	**60.9**	**14.1**	**0.4**

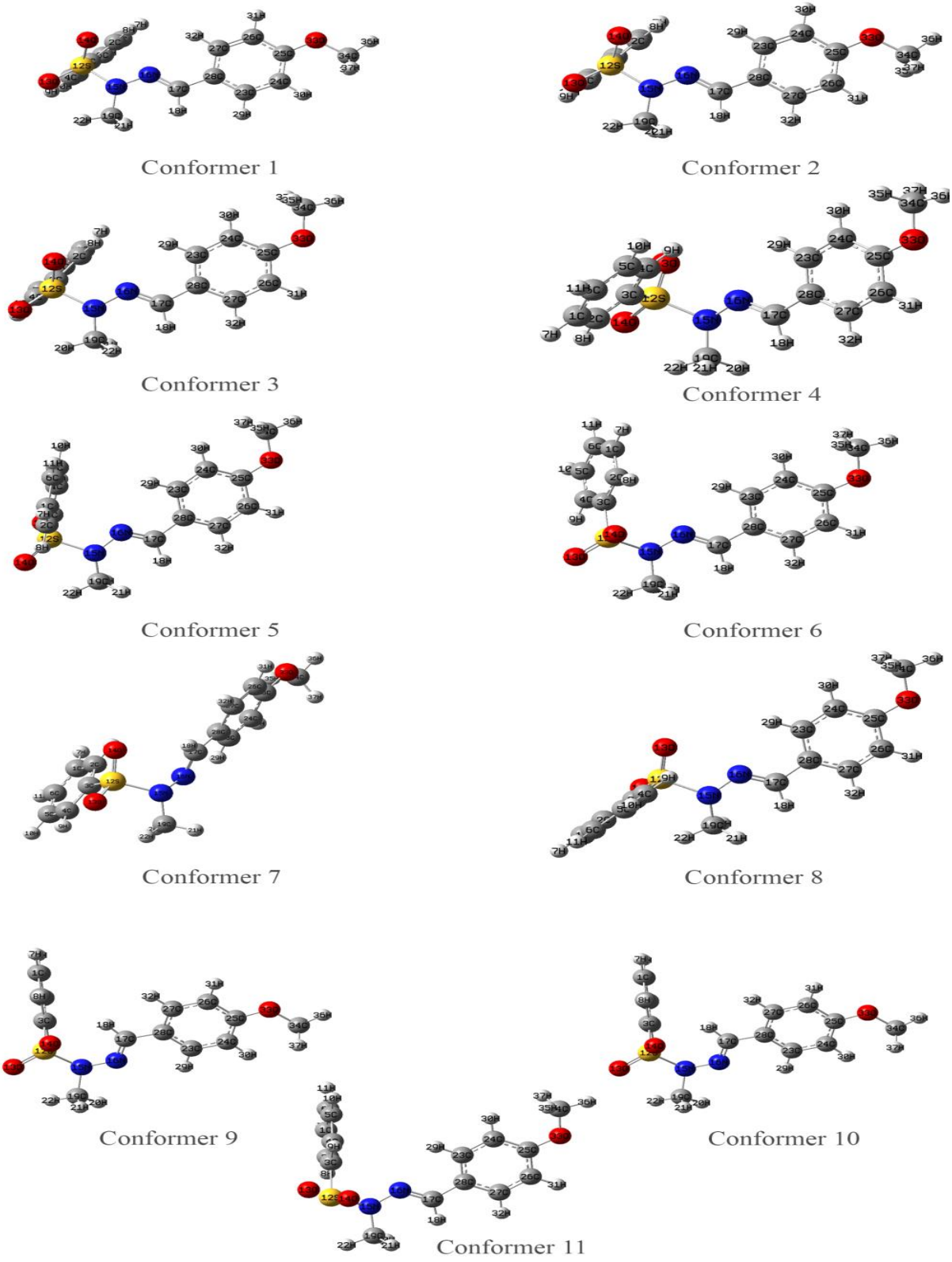

Fig. 3: Geometries of the conformers.

Natural Bond Analysis

The results of the natural bond orbital (NBO) were calculated using the Gaussian 09 program with the DFT/B3LYP method and the 6-31G(d,p), 6-311G(d,p), and LanL2Dz basis sets. NBO calculations offer the opportunity to explore charge intermolecular bonding and the interaction among bonds. A larger stabilization energy value shows greater intensity of the interaction between electron donors and electron acceptors. The natural bond orbital analysis of the obtained molecule is given in Table 4.

NBO analysis was performed on the title compound at the B3LYP/6-31G(d,p), 6-311G(d,p), and LanL2Dz level. The most stable conformer was determined with intra-molecular hydrogen bonding. The highest interaction energies between the LP (1) of N_{16} and BD*(1) of C_{17}-H_{18} were calculated as 11.05, 10.25, and 10.49 kcalmol^{-1} for 6-31G(d,p), 6-311G(d,p), and LanL2DZ, respectively. The second interaction energy E(2) value calculated for the oxygen lone pair N_{15} with anti-bonding $C_{19}H_{20}$ was found to be 6.12 kcal/mol with the B3LYP/6-31G(d,p) basis set. There was a similar interaction between the oxygen lone pair N_{15} and anti-bonding of $C_{19}H_{21.}$ The interaction value was found to be 2.4 kcal/mol. The interaction energy values of the oxygen lone pair O_{33} with anti-bonding C_{34}- $H_{35}$and C_{34}- H_{37} were calculated to be (E2 1.26- 5.44 kcal/mol, and E2(2) 1.25- 5.43 kcal/mol) for the obtained compound, and are presented in Table-3.

NMR calculations

Chemical shifts were reported in ppm relative to TMS for the NMR spectra. The most stable conformer of the obtained molecule was used to calculate the NMR spectra with the B3LYP method at 6-311G(d,p) level using the gauge-including atomic orbital (GIAO) [22] ^{1}H and ^{13}C chemical shift calculations were performed by the B3LYP functional with the 6-31G(d,p), 6-311G(d,p), and LanL2Dz basis sets. The ^{1}H NMR and ^{13}C NMR diagrams of N'-(4-methoxybenzylidene)benzenesulfonohydrazide are presented in Fig. 4. andFig. 5., respectively. The correlation graphs between the experimental and calculated NMR spectra by three different methods are shown in Fig. 6.

From the results regarding the shift of the hydrogen atom, the chemical shifts of H10 and H9 were higher than those of the other hydrogen atoms in the chain. This is purely due to the extended influence on the hydrogen atom by nearby sulfur atoms.

The shifts of the title molecule were calculated at 7.07–8.07 ppm with B3LYP/6-31G(d), at 6.82–7.87 ppm with B3LYP/6-311G(d,p), and at 6.82–7.87 ppm with B3LYP/ LanL2Dz.

Table-3: Theoretical and experimental ^{13}C and ^{1}H chemical shift for the title compound (ppm).

Exp.	6-31G(d,p)	6-311G(d,p)	Lan2-Dz	Δ(Exp.-(6-31G))	Δ(Exp.-(6-311G))	Δ(Exp-(cc-PVDZ))	Atom
114.6	144.8	167.1	150.1	30.1	52.4	35.5	25-C
161.1	129.4	146.9	136.1	31.7	14.2	25.0	3-C
162.1	121.8	139.4	128.3	40.3	22.7	33.8	17-C
126.8	117.1	136.3	123.0	9.7	9.5	3.8	6-C
114.3	116.8	134.7	122.9	2.5	20.4	8.6	23-C
132.0	115.6	134.4	120.0	16.4	2.4	12.0	2-C
114.3	114.7	133.1	119.3	0.4	18.8	5.1	28-C
130.2	113.6	132.6	118.4	16.6	2.3	11.8	1-C
130.1	112.9	131.9	118.2	17.2	1.8	11.9	5-C
132.0	112.3	130.8	117.6	19.7	1.1	14.3	4-C
114.4	112.0	130.6	115.8	2.4	16.2	1.4	27-C
114.5	104.6	122.8	111.2	9.9	8.3	3.3	26-C
114.6	94.6	110.0	98.9	20.0	4.6	15.7	24-C
77.0	43.1	54.3	48.0	33.9	22.7	29.0	34-C
55.4	21.8	30.6	22.2	33.6	24.9	33.2	19-C
7.0	8.5	8.3	8.4	1.5	1.4	1.5	32-H
8.1	8.3	8.0	8.3	0.2	0.0	0.2	8-H
7.8	8.0	7.8	8.0	0.2	0.0	0.2	9-H
7.5	7.6	7.5	7.6	0.1	0.0	0.1	11-H
7.4	7.6	7.4	7.6	0.2	0.1	0.2	10-H
7.3	7.5	7.4	7.6	0.2	0.1	0.2	7-H
6.9	7.1	7.1	7.3	0.2	0.2	0.4	31-H
7.0	7.1	7.0	7.0	0.1	0.1	0.0	29-H
8.8	6.9	6.9	6.9	1.9	1.9	1.9	18-H
6.8	6.7	6.5	6.4	0.1	0.3	0.4	30-H
2.2	4.3	4.2	4.2	2.1	2.0	1.9	22-H
4.1	4.1	4.0	3.8	0.0	0.1	0.2	36-H
3.7	3.7	3.5	3.4	0.0	0.2	0.3	37-H
3.5	3.7	3.5	3.4	0.2	0.0	0.1	35-H
2.2	3.0	2.8	2.7	0.8	0.6	0.5	21-H
2.1	2.0	1.8	1.5	0.0	0.3	0.5	20-H

Table-4: Natural Bond Orbital analysis of the title compound.

Donor NBO (i)	Acceptor NBO(j)	6-31 G(d,p)			6-311 G(d,p)			Lan2-Dz		
		E(2)[a]	E(i)-E(j)[b]	F(i,j)[c]	E(2)[a]	E(i)-E(j)[b]	F(i,j)[c]	E(2)[a]	E(i)-E(j)[b]	F(i,j)[c]
LP (3) O13	**BD*(1) C19 – H22**	**1.24**	**0.75**	**0.029**	**0.67**	**0.71**	**0.02**	**1.02**	**0.78**	**0.026**
LP (2) N15	**BD*(1) C19 – H20**	**6.12**	**0.73**	**0.063**	**6.15**	**0.69**	**0.06**	**6.45**	**0.75**	**0.065**
LP (1) N15	**BD*(1) C19 – H21**	**2.4**	**0.74**	**0.04**	**3.05**	**0.69**	**0.043**	**2.67**	**0.76**	**0.043**
LP (1) N16	**BD*(1) C17 – H18**	**11.05**	**0.81**	**0.086**	**10.25**	**0.78**	**0.081**	**10.49**	**0.81**	**0.084**
LP (1) O33	**BD*(1) C34 – H35**	**1.26**	**0.97**	**0.031**	**0.74**	**0.92**	**0.023**	**1.04**	**0.97**	**0.028**
LP (1) O33	**BD*(1) C34 – H36**	**1.84**	**1.00**	**0.039**	**3.02**	**0.94**	**0.048**	**2.18**	**1.01**	**0.042**
LP (1) O33	**BD*(1) C34 – H37**	**1.25**	**0.97**	**0.031**	**0.73**	**0.92**	**0.023**	**1.02**	**0.97**	**0.028**
LP (2) O33	**BD*(1) C34 – H35**	**5.44**	**0.74**	**0.059**	**5.72**	**0.69**	**0.058**	**5.37**	**0.75**	**0.059**
LP (2) O33	**BD*(1) C34 – H37**	**5.43**	**0.74**	**0.059**	**5.69**	**0.69**	**0.058**	**5.35**	**0.75**	**0.059**

[a] E(2) means energy of hyperconjugative interactions.(kcal/mol)
[b] Energy difference between donor and acceptor i and j NBO orbitals.(a.u)
[c] F(i, j) is the Fock matrix element between i and j NBO orbitals.(a.u)

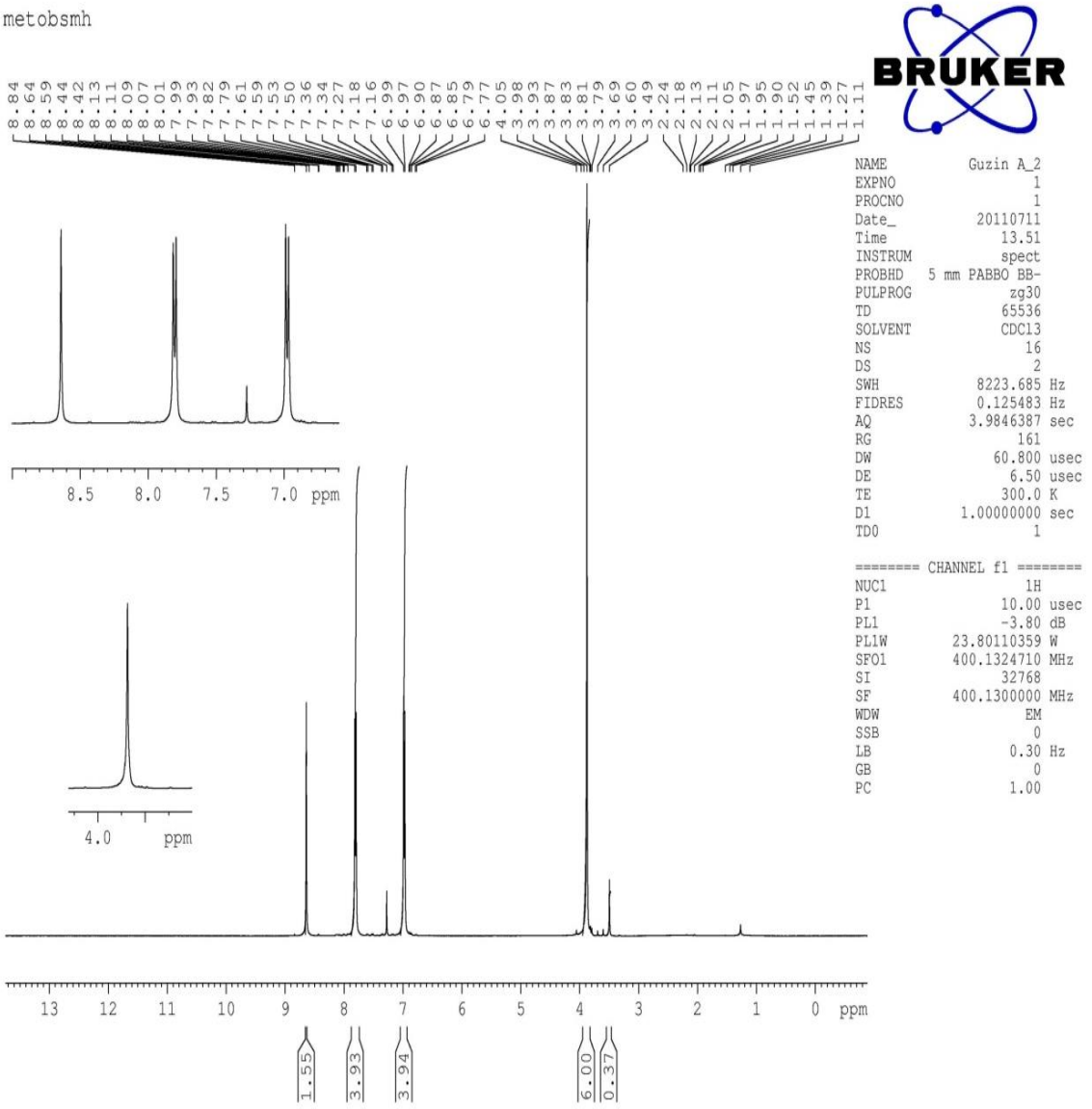

Fig. 4: Experimental ^{1}H NMR chemical shift spectrum of the obtained molecule.

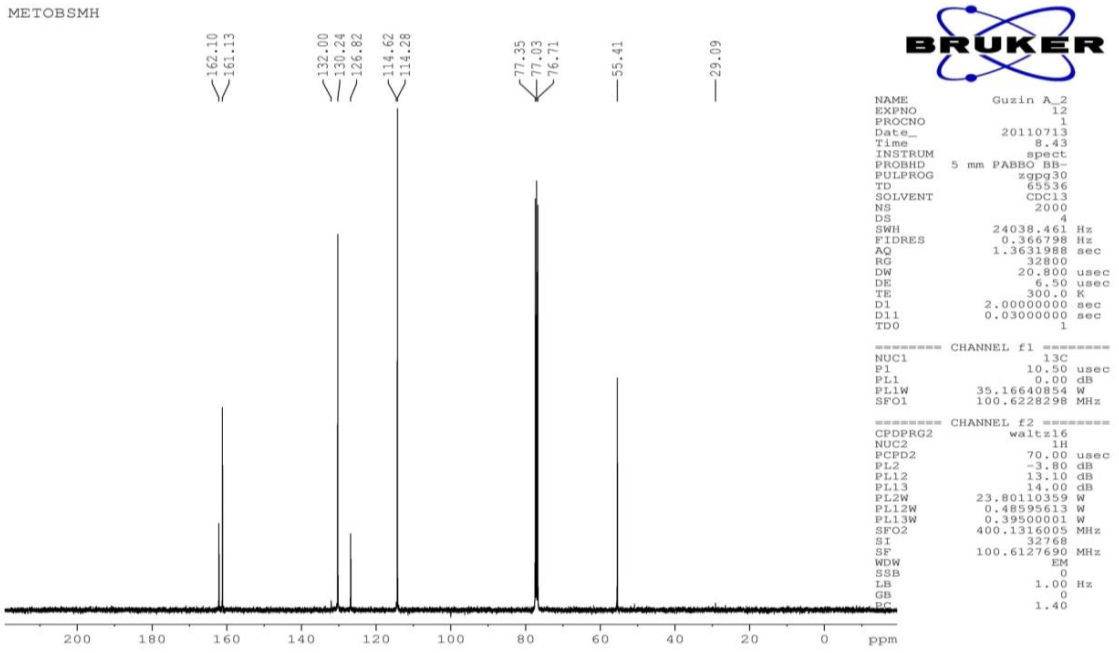

Fig. 5: Experimental ^{13}C NMR chemical shift spectrum of the obtained molecule.

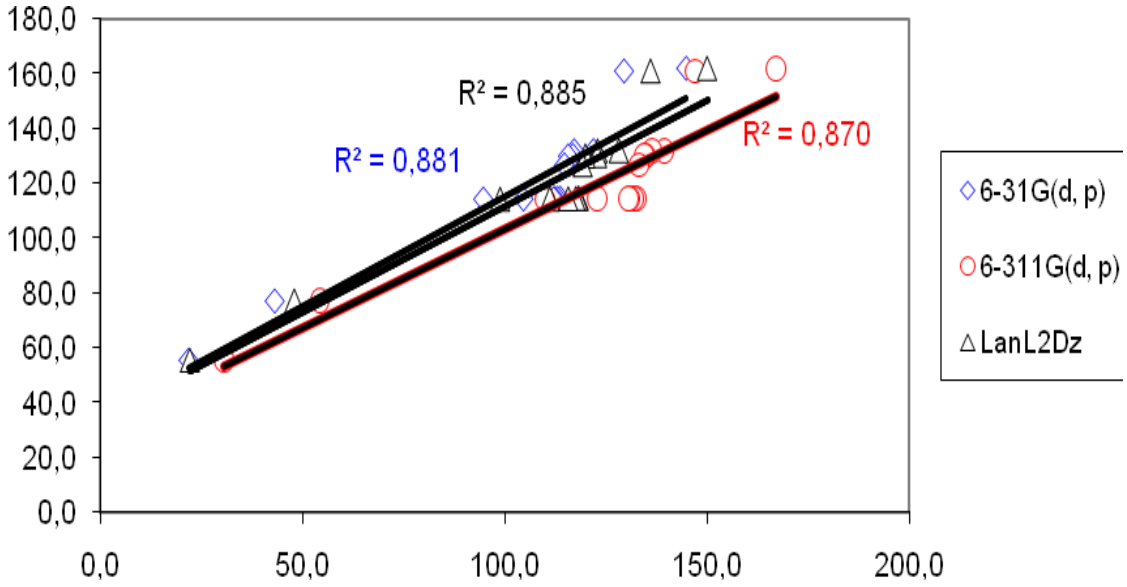

Fig. 6: Calculated and experimental NMR Spectra of the title compound.

HOMO-LUMO analysis

The HOMO–LUMO analysis for the title compound was calculated at the B3LYP/6-31G(d,p) level. The frontier molecular orbital is seen in Fig7.

HOMO–LUMO helps to characterize the chemical reactivity and kinetic stability of the molecule [24]. The HOMO orbital is concentrated on the methoxybenzene ring and sulfonyl groups. This means that electrophilic attack occurs here. The LUMO orbital is located over the sulfonyl group's

benzene ring; for this reason, nucleophilic attack occurs here. The LUMO orbital is also slightly located over the methoxy group. The HOMO and LUMO energy gap value is 3.81 eV. A small energy gap value is polarized and is known as a soft molecule. This energy gap value explains the eventual charge transfer interactions taking place.

An atom occupied by more densities of HOMO should have a stronger ability for donor electrons, whereas an atom occupied by more densities of LUMO should have a stronger ability to attract electrons.

Molecular electrostatic potential

The molecular electrostatic potential (MEP) gives information about the net electrostatic effect produced at that point by the total charge distribution of the compound and correlates with the chemical reactivity of the compounds. The molecular electrostatic potential (MEP) of the obtained molecule is illustrated in Fig8.

Maps help provide understanding of the relative polarity of a molecule. The different values of electrostatic potential on the surface are represented by different colors. Electrostatic potential shows an increase from red to blue. The red regions represent the most negative potential, blue represents regions of the most positive potential, and green represents regions of zero potential. Regions of negative potential are usually associated with alone pair of electronegative atoms. As seen from the MEP map of the title molecule, the orange regions are localized over C=O groups and N atoms. The yellow region, which has positive potential, is located over the phenyl rings.

Vibrational Analysis

The title compound has 37 atoms and is expected to have 106 normal modes of fundamental vibrations. The normal mode analyses are provided in Table 5.The experimental and theoretical spectra are shown inFig9.

The vibrational frequencies calculated with the DFT method with the 6-31G(d,p), 6-31G(d,p),and LanL2DZ basis sets were scaled by 0.961, 0.967, and 0.961 for wave numbers greater than 1700 cm^{-1}, respectively. The values of the DFT calculations enabled good agreement with the experimentally recorded organic compounds when the vibrational harmonic frequencies were scaled using the scale factor. This was obtained by considering systematic errors; basis set deficiencies, and anharmonicity [25-29]. After the calculated wave numbers were scaled, the deviation from the experiments was less than 10 cm^{-1}. The correlation graph of the calculated and experimental wave numbers is shown in Fig 10.

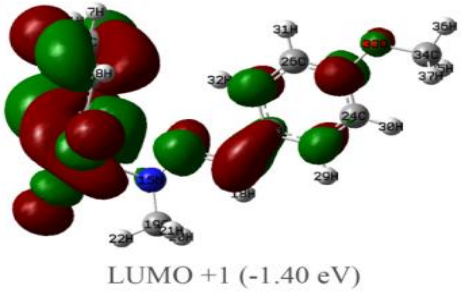

LUMO +1 (-1.40 eV)

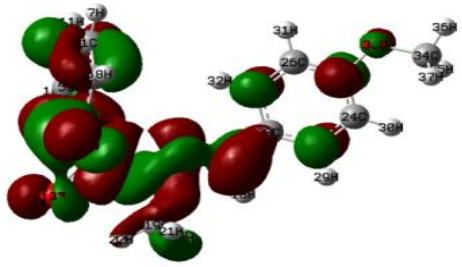

LUMO(-1.98eV)

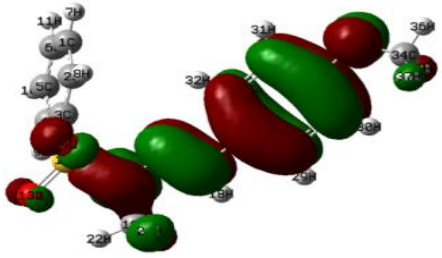

HOMO (-5.80 eV)

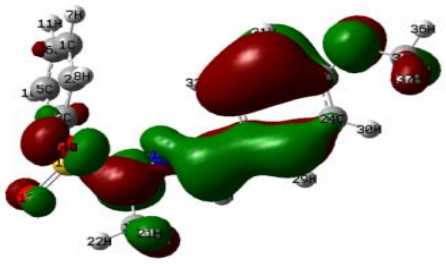

HOMO -1 (-7.15eV)

Fig. 7: The frontier molecular orbital pictures of the most stable conformer.

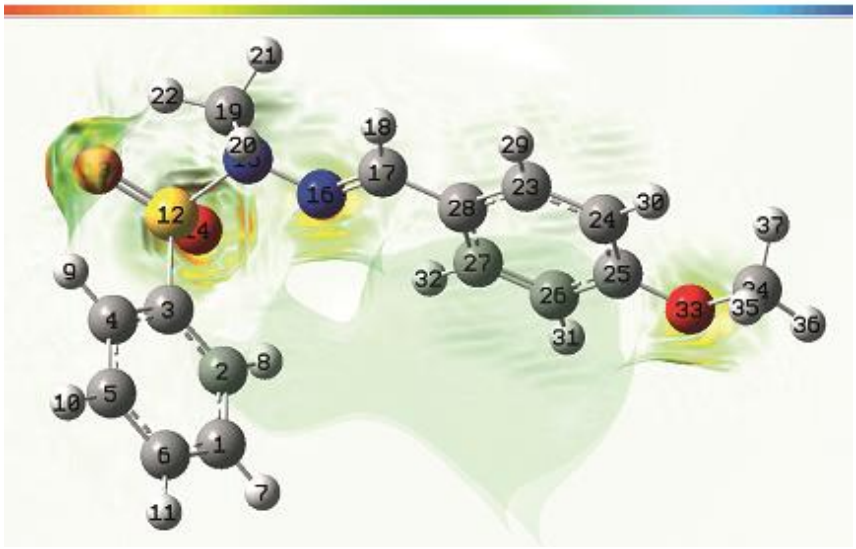

Fig. 8: MEP of the obtained molecule.

CH vibrations

The title compound consists of an aromatic ring system and sulfonyl hydrazine. The C-H stretching vibration of the benzene ring appears in the region 3000–3100 cm^{-1}, which is the characteristic region of C-H stretching vibration [30]. The stretching vibrations of the C-H methyl group were localized and observed in the range 3000–2800 cm^{-1} [31].

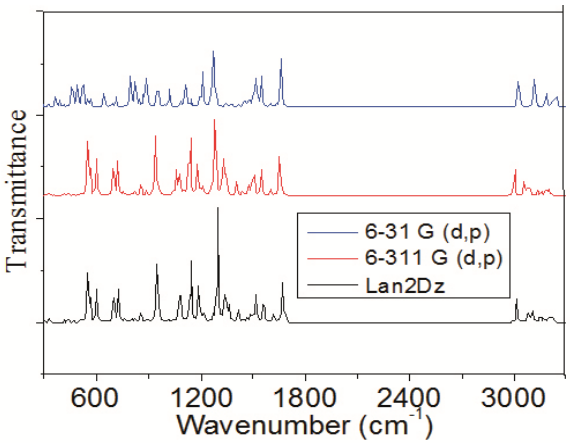

Fig. 9: Calculated IR Spectra of the title compound.

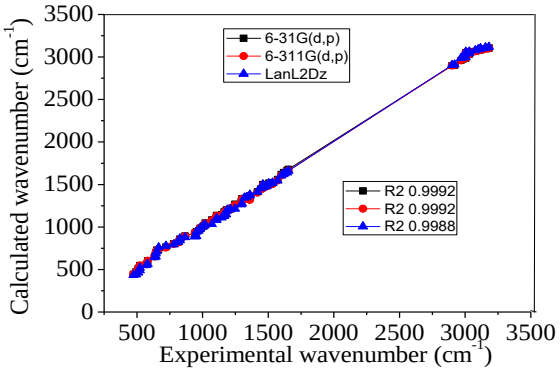

Fig. 10: Calculated and experimental IR Spectra of title compound.

The C-H stretching vibrations of the obtained molecule were observed at 3181, 3154, 3117, 3098, 3076, 3032, 3030, 3005 cm^{-1} in the IR spectrum and calculated at 3109- 3100, 3098-3095, 3084-3081, 3075, 3065-3064, 3051, 3029 cm^{-1} by 6-31G(d,p), at 3110- 3100, 3098-3096, 3086-3081, 3076, 3065-3064, 3051, 3029 $cm^{-1}$by 6-311G(d,p) 3117, and at 3112-3107, 3101-3097, 3091, 3078-3064, 3062, 3042 cm^{-1} by LanL2Dz with the contribution and were acquired at 100% on the PED table. The bands were found at 2968, 2920, 2900 cm^{-1} in the title compound and calculated at 2960, 2900, 2898 $cm^{-1}$by 6-31G(d,p), at 2960, 2903, 2898 cm^{-1} by 6-311G(d,p) and at 2989, 2912, 2905 cm^{-1} by LanL2Dz, and are ascribed to CH_3 stretching vibrations.

The H-C-H in-plane bending vibrations appear as a medium band in the IR spectrum at 1532-1443 cm^{-1}. These vibrations were calculated at 1519-1447 cm^{-1}. The C-H out-of-plane bending vibrations are coupled vibrations and occur in the region 1000–750 cm^{-1} [32, 33]. The aromatic C-H out-of-plane bending vibrations were calculated at 945-729 and were observed at 954- 652 cm^{-1} in the IR spectrum.

C=C vibrations

The C=C stretching vibrations normally appear around 1650- 1400 cm^{-1} in an aromatic compound. These four peaks confirm that the compound is aromatic in nature [34]. The C=C stretching vibrations of the obtained molecule were found at 1680- 1560 cm^{-1} and were also observed at 1664-1545 cm^{-1} in the IR spectrum.

CCC bending bands always occur at~600 cm^{-1} [35]. The CC in -plane bending vibrations appeared at 1361,1071,1021, 644, 634 cm^{-1}, whereas the out -of -plane bending vibrations were observed at 954, 721, 666, 644, 522, 493 cm^{-1} In the title molecule, the computed values found as 1364-1361, 1074,1047, 694,652-627 cm^{-1} by the 6-31G(d,p) basis set, as 1319-1343, 1061,1042, 691,652-628 $cm^{-1}$by the 6-311G(d,p) basis set and as 1380-1371, 1061,1029, 652, 643-624 cm^{-1} by the LanL2Dz basis set were assigned to CCC bending vibrations.

Table-5: Normal coordinate analysis of the title compound.

No.	Exp.	6-31G(d,p)	6-311G(d,p)	Lan2-Dz	% PED	Assignment
1	3181	3109	3110	3117	87 C_2H	ν C_1H
2	3181	3100	3100	3117	87 C_4H	ν C_1H
3	3154	3098	3098	3112	76 $C_{24}H$ + 21 $C_{23}H$	ν C_2H
4	3154	3095	3096	3107	92 $C_{27}H$	ν C_2H
5	3117	3084	3086	3101	97 C_6H	ν C_1H
6	3117	3081	3081	3097	98 $C_{27}H$	ν C_2H
7	3098	3075	3076	3091	78 C_5H + 22 C_1H	ν C_2H
8	3076	3065	3065	3078	98 $C_{19}H$	ν c_AH
9	3076	3064	3062	3064	86 C_6H	ν C_1H
10	3032	3051	3054	3062	88 $C_{23}H$	ν C_2H
11	3030	3029	3032	3042	81 $C_{34}H_{35}$ + 12 $C_{34}H_{37}$	ν $C_{mo}H$
12	3005	2985	2985	2997	78 $C_{17}H$ + 10 $C_{19}H$	ν CH
13	2984	2975	2975	2994	100 $C_{19}H$	ν CH
14	2968	2960	2960	2989	90 $C_{34}H$	ν $C_{mo}H$
15	2920	2900	2903	2912	91 $C_{34}H$	ν $C_{mo}H$
16	2900	2898	2898	2905	94 $C_{19}H$	ν C_mH
17	1654	1680	1664	1661	65 C_{17}=N +13$N_{16}C_{17}H$	ν CN
18	1644	1667	1651	1642	72 $C_{26}C_{27}$ + 10 $C_{23}C_{24}$	ν C_2C
19	1626	1641	1626	1636	56 C_4C_5	ν C_1C
20	1617	1640	1625	1622	52C_5C_6 + 28 C_2C_3 + 10 C_3C_4	ν C_1C
21	1599	1620	1605	1605	58 $C_{27}C_{28}$ + 10 $C_{17}N$	ν C_2C
22	1572	1560	1545	1546	40 $C_{26}C_{27}$ + 27 $C_{23}C_{24}H_{30}$	ν C_2C
23	1532	1519	1507	1519	77 $HC_{19}H$	δ HC_mH
24	1532	1518	1505	1518	77 $HC_{34}H$	δ $HC_{mo}H$
25	1505	1517	1504	1514	83 $HC_{19}H$	δ HC_mH
26	1505	1505	1492	1507	82 $HC_{34}H$	δ $HC_{mo}H$
27	1459	1501	1491	1501	60 $HC_{19}H$	δ HC_mH
28	1487	1487	1477	1484	81 $HC_{34}H$	δ $HC_{mo}H$
29	1487	1487	1477	1478	60 C_1C_6H + 29 C_1C_2	δ $HC_{Gal}H$
30	1459	1468	1455	1466	64 $C_{24}C_{23}H$ + 10 $C_{26}C_{27}$	δ HC_2C_2
31	1443	1447	1441	1455	65 $HC_{19}H$ + 10 $C_{28}C_{17}H$	δ HC_mH
32	1418	1414	1403	1414	46 $C_{28}C_{17}H$ + 10 $HC_{19}H$	δ HC_2C_a
33	1361	1364	1319	1380	77 $C_1C_2C_3$	δ $C_1C_1C_1$
34	1361	1361	1343	1371	58 $C_{23}C_{24}C_{25}$	δ $C_2C_2C_2$
35	1335	1344	1333	1352	65 OS_{12}	δ OSO
36	1319	1337	1329	1345	58 C_3C_4H	δ C_1C_1H
37	1300	1334	1328	1278	30 $C_{26}C_{27}H$+ 13 $C_{23}C_{24}H$	δ C_2C_2H
38	1295	1298	1280	1265	37 $C_{33}O_{25}$+ 17 $C_{17}C_{28}$	ν OC_{mo}
39	1247	1269	1260	1214	62 $HC_{17}C_{28}$+ 14 $C_{17}C_{28}$	δ CC_aH
40	1211	1220	1213	1211	43 $HC_{19}H$ + 14 $S_{12}C_{15}$	δ sHC_mH
41	1211	1211	1204	1206	75 $HC_{34}H$ + 14 $O_{34}C_{35}$	δ $HC_{mo}H$
42	1184	1204	1199	1195	58 C_4C_5H	δ HC_1C_1
43	1184	1198	1190	1192	67 $C_{26}C_{27}H$	δ HC_2C_2
44	1179	1190	1185	1150	85 C_5C_6H	δ HC_1C_1
45	1179	1189	1181	1147	41 C_{17}NN+ 13 C_5C_6H +13 $C_{26}C_{27}H$	δ $HC_{Gal}C$
46	1164	1177	1170	1130	31 $HC_{34}H$ +30 $C_{25}O_{33}C$	δ $HC_{mo}H$ +δ COC
47	1147	1147	1138	1111	43 C_3S +30 $O_{13}SO$	ν CS
48	1107	1138	1132	1106	53 $C_{26}C_{27}H$ + 30 $C_{23}C_{24}O$	δ C_2C_2H +δ COC
49	1107	1132	1125	1081	64 $HC_{19}H$ +21 $N_{15}C_{19}$	δ HC_mH
50	1100	1105	1100	1050	60 $C_2C_1C_6$	δ $C_1C_1C_1$
51	1071	1085	1078	1034	52 C_3S_{12}+21 C_2C_3	ν CS
52	1071	1074	1061	1029	47 $C_{23}C_{24}C_{25}$ + 19 $O_{33}C_{34}$	δ $C_2C_2C_2$
53	1021	1047	1042	1028	62 $C_1C_6C_5$ + 11 C_3S	δ $C_1C_1C_1$

54	**1021**	**1026**	**1023**	**1027**	**77 τ($C_{26}C_{27}$)**	**τ C_2C_2**
56	**1008**	**1008**	**1011**	**1008**	**68 τ(C_1C_6) + 11 C_1C_6**	**τ C_1C_1**
57	**983**	**987**	**992**	**990**	**75 τ($C_{26}C_{27}$)**	**τ C_2C_2**
58	**983**	**982**	**988**	**979**	**85 τ(C_4C_5)**	**τ C_1C_1**
59	**970**	**959**	**959**	**956**	**59 τ($C_{17}C_{28}$) + 14 τ($C_{23}C_{24}$)**	**τ C_2C_a**
60	**954**	**947**	**941**	**945**	**82 $N_{15}N_{16}$ + 12 $C_{19}N$**	**ν NN**
61	**954**	**941**	**937**	**892**	**20 τ(C_1C_2) + 18 P(C_4)**	**τ C_1C_1+ γ (C_1)**
62	**942**	**928**	**930**	**887**	**60 τ($C_{17}C_{28}$) + 37 τ($C_{23}C_{24}$)**	**τC_1C_1+ τC_2C_2**
63	**867**	**896**	**891**	**880**	**59 $C_{23}C_{28}$ + 21 $C_{26}C_{27}$**	**ν C_2C_2**
64	**828**	**859**	**856**	**866**	**40 τ(C_1C_2) + 11 τ(C_4C_5)**	**ν C_1C_1**
65	**828**	**854**	**853**	**844**	**41 τ($C_{26}C_{27}$) + 33 τ(C_4C_5)**	**τC_1C_1+ τC_2C_2**
66	**815**	**820**	**817**	**822**	**41 τ($C_{26}C_{27}$) + 39 τ($C_{23}C_{24}$)**	**τC_2C_2**
67	**780**	**804**	**800**	**795**	**47 $C_{23}C_{28}C_{27}$+ 19 $C_{25}O_{33}C_{34}$**	**δ$C_2C_2C_2$ +δC_2OC_{mo}**
68	**721**	**766**	**758**	**777**	**34 τ(C_5C_6)+ 30 P(C_3)**	**τ C_1C_1+ γ (C_1)**
69	**666**	**732**	**738**	**760**	**45 P(C_{28})+ 29 P(C_{25})**	**γ(C_2) + γ(C_2)**
70	**652**	**729**	**725**	**712**	**41 τ(C_3C_4) + 39 C_3S_{12}**	**τ C_1C_1+ ν (CS)**
71	**644**	**698**	**698**	**688**	**51 P(C_1)+ 16 P(C_5)**	**γ(C_1)**
72	**644**	**694**	**691**	**652**	**52 $C_1C_5C_6$ + 27 C_3S_{12}**	**δ$C_1C_1C_1$**
73	**634**	**652**	**652**	**643**	**18 $C_{24}C_{23}C_{28}$+ 13 $C_{27}C_{26}C_{25}$**	**δ$C_2C_2C_2$**
74	**630**	**627**	**628**	**624**	**60 $C_1C_2C_3$+ 36 $C_4C_5C_6$**	**δ$C_1C_1C_1$**
75	**583**	**604**	**604**	**565**	**17 τ($N_{15}N_{16}$)+ 16 τ($N_{25}S_{33}$) + 0τ($C_{17}C_{28}$)**	**τ NN+ τ NS**
76	**571**	**562**	**561**	**550**	**70 $O_{13}S_{23}O_{14}$+ 15 $C_{25}O_{33}C$**	**δ OSO**
77	**522**	**548**	**547**	**520**	**47 τ($N_{15}N_{16}$)+ 13τ($C_{17}C_{28}$) + 10τ($C_{23}C_{24}$)**	**τ NN**
78	**522**	**545**	**542**	**490**	**48 P(C_{28})+ 13 P(C_{25})**	**γ(C_2) + γ(C_2)**
79	**510**	**511**	**510**	**463**	**35 τ($S_{12}N_{15}$)+ 13 τ($C_{25}C_{33}C_{34}$)**	**τ SN**
80	**493**	**473**	**471**	**440**	**36 P(C_3)+ 13 P(C_6)**	**γ(C_1)**
81	**474**	**446**	**444**	**434**	**30 τ($N_{15}N_{16}$)+ 10 $C_{25}O_{33}C_{24}$**	**τ NN**

*ν*Stretching, *δ* in-plane, *γ* out-of-plane, *τ*–torsion C atoms; C_A:A ring, C_B: B ring, C_C:C ring, C_Q: quercetin ring-, C_{Gal}: galactoside ring.

S=O, C-S Vibrations

The SO_2 stretching vibrations occur in the region 1125–1150 and 1295–1340 cm^{-1}[21].The bands appeared at 1335 cm^{-1} in IR and were calculated at 1344 cm^{-1} by the 6-31G(d,p) basis set at 1333 cm^{-1} by the 6-311G(d,p) basis set, and at 1352 cm^{-1} by the LanL2Dz basis set. In a recent study, the SO_2 in-plane bending vibrations were found at 590 cm^{-1} for a benzenesulfonic acid methyl ester structure [21]. In this paper, the δ OSO in-plane bending vibration was observed at 571 cm^{-1} and calculated at 562 cm^{-1} by the 6-31G(d,p) basis set, at 561 cm^{-1} by the 6-311G(d,p) basis set, and at 550 cm^{-1} by the LanL2Dz basis set.

Normally, the C–S stretching bands are observed in the range of 930–670 cm^{-1} [33,34]. For the title molecule, the C–S stretching vibration was observed at 1147 cm^{-1} (30% contribution δ OSO in-plane bending vibration), and at 1071 cm^{-1}in IR diagram; this agrees well with the calculated stretching vibration at 1147 and 1085 cm^{-1} by the B3LYP/6-31G(d,p) method, at 1138 and 1078 $cm^{-1}$by the B3LYP/6-31G(d,p) method and at 1111 and 1034 cm^{-1} by the B3LYP/LanL2Dz method.

C=N, O-CH_3 Vibrations

The C-N stretching usually lies in region 1400-1200 cm^{-1} [33, 34].

The stretching vibration of the C=N group in the title molecule was observed at 1654 cm^{-1} and was calculated with a 65% contribution of the C=N stretching force constant and calculated at 1664 cm^{-1} by the 6-311G(d,p) basis set and at 1661 cm^{-1} by the LanL2Dz basis set.

The O–CH_3 stretching mode is normally assigned in the region 1000–1150 cm^{-1} and the O–CH_3 bending mode is assigned at 310 cm^{-1}[33-35]. The OC band was observed at 1295 cm^{-1} and calculated at 1298 $cm^{-1}$by the 6-31G(d,p) basis set, at 1280 $cm^{-1}$by the 6-311G(d,p) basis set and at 1265 cm^{-1} by the LanL2Dz basis set. The $C_{25}O_{33}C$ in-plane bending was observed at 1164 cm^{-1} and calculated at 1177 $cm^{-1}$by the 6-31G(d,p) basis set, at1170 cm^{-1} by the 6-311G(d,p) basis set and at 1130 cm^{-1} by the LanL2Dz basis set.

Conclusion

In this present study the conformer analysis were performed to find the most stable conformer. 11 conformational isomers were obtained in gaseous phases. The most important difference between conformers is found to be the replacement of the benzene ring and -OCH_3 groups.

The potential energy curves around the flexible bonds of N'-(4-methoxybenzylidene) benzenesulfonohydrazide was performed. The highest rotational barrier 48 kcal/mol for N15N16C17H18torsiyonal angles. This is an expected result because the rotation around the double bond is difficult. The lowest rotational barrier 3 kcal/mol for N16N15C19H21torsiyonal angles.

The dipole moment values of the determined conformers in the gas phase vary between 4.06 Debye (conformer 11) and 7.03 Debye (conformer 2).

NBO analysis was performed on the title compound at the B3LYP/6-31G(d,p), 6-311G(d,p), and LanL2Dz level. The most stable conformer was determined with intra-molecular hydrogen bonding. The highest interaction energies between the LP (1) of N16 and BD*(1) of C17-H18 were calculated as 11.05, 10.25, and 10.49 kcal/mol for 6-31G (d,p), 6-311G(d,p), and LanL2DZ, respectively. The second interaction energy E (2) value calculated for the oxygen lone pair N15 with anti-bonding C19H20 was found to be 6.12 kcal/mol with the B3LYP/ 6-31G(d,p) basis set.

Based on the DFT calculations at B3LYP/6-31G(d,p), B3LYP/6-311G (d,p), and B3LYP /LanL2Dz levels, all the properties of the synthesized title molecule were investigated by FT-IR and NMR spectroscopy. FT-IR diagrams were theoretically drawn in three ways. Experimental data and theoretical data were compared in the graph. Thus, it was determined that the R2 values of the graphs obtained with 6-31 G(d,p) and 6-311 G(d,p) methods were closer to the real result. Also, the optimized bond length, bond angle, and dihedral angles were calculated and compared by different DFT methods. The PES of the obtained molecule was calculated by DFT/6-31G(d,p). Among the eleven conformers in the gas phase, the most stable conformer was determined by a relaxed scan through 8 dihedral angles. The strong hyper conjugative interaction energy values were calculated between the LP (N16) atom and BD* (C17-H18) bond. The HOMO–LUMO energy gaps were calculated at 3.82 eV for conformer 1. In general, compounds having a HOMO-LUMO gap of 1.5 eV or less are considered to be chemically active [36]. The HOMO-LUMO gap value of our compound, 3.82 eV, shows that its chemical activity is weak.

Acknowledgements

In this study, all calculations were calculated at TUBİTAK ULAKBİM, (TR-Grid e-Infrastructure).

References

1. R. Bentley, Different roads to discovery; Prontosil (hence sulfa drugs) and penicillin (hence β-lactams), *J. Ind. Microbiol.Biotechnol*.,**36**,775 (2009)
2. E.P. Abraham, E. Chain, C.M. Fletcher, H.W. Florey, A.D. Gardner, N.G. Heatleyand M.A. Jennings, Further observations on penicillin. *Lancet.*,**2**,177 (1941**)**.
3. K. Henryand M. D. Beecher, Ethics and clinical Research, *N Engl J Med.*, **274**, 1354 (1966).
4. S.M. Sondhi, M. Johar, N. Singhal, S.G. Dastidar, R. Shuklaand R. Raghubir, Synthesis and anticancer, antiinflammatory and analgesic activity evaluation of some sulfa drug and acridine derivatives, *Monatsh. Chem.*,**131**, 511 (2000).
5. H. E. Lebovitzand M. N. Feinglos, Sulfonylurea drugs: mechanism of antidiabetic action and therapeutic usefulness, *Diabetes care.*,**1**,189 (1978).
6. A. Hanafy, J. Uno, H. Mitaniand Y. Kang, In vitro antifungal activities of sulfa drugs against clinical isolates of Aspergillus and Cryptococcus species, *NihonIshinkin Gakkai Zasshi*.,**48**, 47 (2007).
7. N. Okeke, A. Lamikanraand R. Edelman, Socioeconomic and behavioral factors leading to acquired bacterial resistance to antibiotics in developing countries, *Emerging Infect. Dis*.,**5**,18 (1999).
8. J. H. Lee, H. K. Park, J. Heo, T.O. Kim, G.H. Kim, D.H. Kang, G.A. Song, M. Cho, D.S. Kim, H. W. Kimand C.H. Lee, Drug rash with Eosinophilia and systemic symptoms (DRESS) syndrome induced by celecoxib and anti-tuberculosis drugs, *J. Korean Med. Sci.*,**23**,521 (2008).
9. Y.S. Huang, H.D. Chern, W.J. Su, J.C. Wuand S.L. Lai, Polymorphism of the N-acetyltransferase 2 gene as a susceptibility risk factor for antituberculosis drug–induced hepatitis, *Hepatology*.,**35**,883 (2002).
10. K.S. Jain, T.S. Chitre, P.B. Miniyar, M.K. Kathiravan, V.S. Bendre, V.S. Veer, S.R. Shahaneand C. J. Shishoo, Biological and medicinal significance of pyrimidines, *Curr. Sci.*,**90**,793 (2006).
11. K. Bharatham, N. Bharatham, K. H. ParkandK.W. Lee, Binding mode analyses and pharmacophore model development for sulfonamidechalcone derivatives, a new class of α-glucosidase inhibitors, *J. Mol. Graph. Model*.,**26**,1202 (2008).
12. Q. Liang, Q. Wang, S.F. Xuand Y.X Sun,Experimental and theoretical studies on bis [μ-2-methoxy-N′-(2-oxidobenzoyl) benzohydrazidato (3-)] dipyridinetricopper (II), *Struct. Chem*.,**19**, 279 (2008).

13. H.G. Aslan, Synthesis, structural characterization and DTA/TG studies of a Schiff base, *SDUJ. Nat. Appl. Sci*.,**21**,812 (2017).
14. H.G. Aslan, S. Özcanand N. Karacan, Synthesis, characterization and antimicrobial activity of salicylaldehydebenzenesulfonylhydrazone (*Hsalbsmh*) and its Nickel(II), Palladium(II), Platinum(II), Copper(II), Cobalt(II) complexes, *Inorg. Chem. Commun.*,**14**, 1550 (2011).
15. H.G. Aslan, S. Özcanand N. Karacan, The antibacterial activity of some sulfonamides and sulfonyl hydrazones, and 2D-QSAR study of a series of sulfonyl hydrazones, *Spectrochim. Acta Part A: Molecular and Biomolecular Spectroscopy*.,**98**,329 (2012).
16. M.W. Wong, Vibrational frequency prediction using density functional theory, *Chem Phys Lett.*,**256**,391 (1996).
17. J. Reinhold, R. Benedix, P. Birnerand H. Hennig, Quantum chemical investigations of the π-acceptor ability of α-diimine ligands, *Inor.Chim.Acta*.,**33**,209 (1979).
18. S. Shi, M. A. Gondal, A. A. Al-Saadi, R. Fajgar, J. Kupcik, X.Chang, K. Shen, Q. Xuand Z. S. Seddigi, Facile preparation of g-C_3N_4 modified BiOCl hybrid photocatalyst and vital role of frontier orbital energy levels of model compounds in photoactivity enhancement, *J. Colloid Interface Sci*.,**416**,212 (2014).
19. S. Sebastianand N. Sundaraganesan, The spectroscopic (FT-IR, FT-IR gas phase, FT-Raman and UV) and NBO analysis of 4-Hydroxypiperidine by density functional method, *Spectrochim. Acta Part A: Molecular and Biomolecular Spectroscopy*.,**75**,941 (2010).
20. T. S. Yamuna, J. P.Jasinski,M. Kaur,B. J. Andersonand H. S. Yathirajan, Crystal structure of 3-[4-(pyrimidin-2-yl)piperazin-1-ium-1-yl]butanoate, *ActaCrystallogr. Sect E Struct. Rep. Online*.,**70,** 1063 (2014).
21. H.G. Aslanand N. Karacan, Aromatic sulfonyl hydrazides and sulfonyl hydrazones: antimicrobial activity and physical properties. *Med. Chem. Res*.,**22**,1330 (2013).
22. M. J. Frisch, G. W. Trucks, H. B. Schlegel, G. E. Scuseria, M. A. Robb, J. R. Cheeseman, G. Scalmani, V. Barone, B. Mennucci, G. A. Petersson, H. Nakatsuji, M. Caricato, X. Li, H. P. Hratchian, A. F. Izmaylov, J. Bloino, G..Zheng, J. L. Sonnenberg, M. Hada, M. Ehara, K. Toyota, R. Fukuda, J. Hasegawa, M. Ishida, T. Nakajima, Y. Honda, O. Kitao, H. Nakai, T. Vreven, J. A. Montgomery, Jr., J. E. Peralta, F. Ogliaro, M. Bearpark, J. J. Heyd, E. Brothers, K. N. Kudin, V. N. Staroverov, R. Kobayashi, J. Normand, K. Raghavachari, A. Rendell, J. C. Burant, S. S. Iyengar, J. Tomasi, M. Cossi, N. Rega, J. M. Millam, M. Klene, J. E. Knox, J. B. Cross, V. Bakken, C. Adamo, J. Jaramillo, R. Gomperts, R. E. Stratmann, O. Yazyev, A. J. Austin, R. Cammi, C. Pomelli, J. W. Ochterski, R. L. Martin, K. Morokuma, V. G. Zakrzewski, G. A. Voth, P. Salvador, J. J. Dannenberg, S. Dapprich, A. D. Daniels, O. Farkas, J. B. Foresman, J. V. Ortiz, J. Cioslowski, D. J. Fox, Gaussian 09 Revision A 1 Gaussian Inc. Wallingford CT(2010).
23. A. B. Nielsen, A. J. Holder, *Gaussview Users Reference*, Gaussian Inc, Pittsburg PA. USA(2000-2003).
24. M. H. Jamroz, *Vibrational Energy Distribution Analysis*. Veda 4 Warsaw(2004).
25. J.R. Cheeseman,G.W. Trucks,T.A. KeithandM.J. Frisch, A comparison of models for calculating nuclear magnetic resonance shielding tensors. *J. Chem. Phys.*,**104**, 5497 (1996).
26. J. M. Galbraith, P.R. Schreiner, P. Doz, N. Harris, W. Wei, A. Wittkoppand S. Shaik, A Valence Bond Study of the Bergman Cyclization: Geometric Features, Resonance Energy, and Nucleus-Independent Chemical Shift (NICS).*Values Chem. Eur. J.*,**6**,1446 (2000).
27. İ. Sıdır, Y. GülsevenSıdır, M. Kumalarand E. Taşal, Ab initioHartree–Fock and density functional theory investigations on the conformational stability, molecular structure and vibrational spectra of 7-acetoxy-6-(2,3-dibromopropyl)-4,8-dimethylcoumarin molecule. *J. Mol. Struct*.,**964**,134 (2010).
28. S. Murugavel, P. Jacob, C. S. Stephen, R. Subashini,R. H. Raveendranatha, D. A. Krishnan,. Synthesis, crystal structure investigation, spectroscopic characterizations and DFT computations on a novel 1-(2-chloro-4-phenylquinolin-3-yl)ethanone. *J. Mol. Struct*.,**1122**, 134 (2016).
29. D. N. Sathiyanarayanan, *Vibrational Spectroscopy Theory and Application*, New Age International Publishers, New Delhi, p. 424(2004).
30. D. Lin-Vien, N.B. Colthup, W.G. Fateley and J.G. Grasselli, *The Handbook of Infrared and Raman Characteristic Frequencies of Organic Molecules*, Academic Press,San-Diegop. 241(1991**)**.

31. S. David, P. Babua, S. Periandyb, S. Mohanc, S. Ramalingamdand B.G. Jayaprakashe,.Molecular structure and vibrational investigation of benzenesulfonic acid methyl ester using DFT (LSDA, B3LYP, B3PW91 and MPW1PW91) theory calculations, *Spectrochim. Acta Part A*.,**78**,168(2011).
32. D. Michalska, D. C. Bienko, A. J. A. Bienkoand Z. Latajka,.Density Functional, Hartree−Fock, and MP2 Studies on the Vibrational Spectrum of Phenol,*J. Phys. Chem.*, **100**, 17786 (1996).
33. S.P. Meenakshisundaram, B. Karthikeyan, K. Muthuand S. Sebastian, Molecular structure, spectroscopic (FT-IR, FT-Raman, UV–vis), NBO, thermochemistry analysis of bis(thiourea)zinc(II) chloride crystals, *Mol. Simul.*,**39**,584 (2013).
34. G. Rajaand K. Saravanan, Harmonic Analysis of Vibrations of 4-Chloro-2-Fluroaniline: A Scaled Quantum Mechanical Approach, *Orient J Chem*.,**29**,531 (2013).
35. R. Soleymanı, Y.M. Salehı, T. Yousofzadand A.M. Karımı-Cheshmeh, Synthesis, Nmr, Vibrational And Mass Spectroscopy With Dft/Hf Studies Of 4-(4/-Bromophenyl) -2 mercaptothiazole, *Structure. Orient J Chem*., **28**,627 (2012).
36. P. Udhayakala, A. Jayanthi, T. V. Rajendiran and S. Gunasekaran, Molecular structure, FT-IR and FT-Raman spectra and HOMO LUMO analysis of 2-methoxy -4-nitroaniline using ab initio HF and DFT (B3LYP/B3PW91) calculations, *Appl. Sci. Res*.,**3**,424 (2011).
37. B. Kesimli and A. Topacli, Infrared studies on Co and Cd complexes of Sulfamethoxazole, *Spectrochim. Acta*.,**57**,1031 (2001).